

Supporting Information

Ag-CoO nanocomposites for gas phase oxidation of alcohols to aldehydes and ketones: Intensified O₂ activation at Ag-CoO interfacial sites

Kun Liu^a, Yichen Zhao^a, Jiale Wang^a, Qingsong Xue^{b*}, and Guofeng Zhao^{b*}

^aInstitute of optical functional materials for biomedical imaging, School of Chemistry and Pharmaceutical Engineering, Shandong First Medical University & Shandong Academy of Medical Sciences, Taian, 271016, China

^bShanghai Key Laboratory of Green Chemistry and Chemical Processes, School of Chemistry and Molecular Engineering, East China Normal University, Shanghai 200062, China

*Corresponding authors: qsxue@chem.ecnu.edu.cn (Qingsong Xue),

gfzhao@chem.ecnu.edu.cn (Guofeng Zhao)

Table S1. Specific surface areas of these fresh samples.

Catalyst	Ti-powder	3Ag/Ti-powder	3Ag-3Co ₃ O ₄ /Ti-powder
SSA ^a (m ² /g)	1.2	1.3	1.3

^aSSA: specific surface area.

Table S2. Comparison of the catalysts.

Catalyst	T ^a	WHSV	Ag loading	SSA ^b	D _{Ag} ^c	Conv. ^d	Sel. ^e
	(°C)	(h ⁻¹)	(wt%)	(m ² /g)	(nm)	(%)	(%)
Ag/Ni-fiber [1]	380	20	9.7	-	200-300	92	87
Ag/HMS [2]	320	12.5	2.8	605	5-10	99	96
Ag/SiO ₂ [3]	320	20	1.0	297	-	80	~100
Ag/Ni-fiber-M [1]	300	20	9.9	-	10*100	97	97
Ag _{2.5} Cu ₅ SiC [4]	280	20	2.5	0.2	30-70	99	99
Ag/CaO [3]	240	20	1.0	-	-	22	~100
Ca-Ag/SiO ₂ [5]	240	20	1.0	200	-	66	~100

^aReaction temperature; ^bSpecific surface area; ^cParticle size of Ag; ^dBenzyl alcohol conversion; ^eBenzaldehyde selectivity.

[1] M. Deng, G. Zhao, Q. Xue, L. Chen, Y. Lu, *Appl. Catal. B: Environ.*, **2010**, 99, 222-228.

[2] J. Jia, S. Zhang, F. Gu, Y. Ping, X. Guo, Z. Zhong, F. Su, *Micropor. Mesopor. Mat.*, **2012**, 149, 158-165.

[3] R. Yamamoto, Y. Sawayama, H. Shibahara, Y. Ichihashi, S. Nishiyama, S. Tsuruya, *J. Catal.*, **2005**, 234, 308-317.

[4] L. Zhao, L. Kong, C. Liu, Y. Wang, L. Dai, *Catal. Commun.*, **2017**, 98, 1-4.

[5] Y. Sawayama, H. Shibahara, Y. Ichihashi, S. Nishiyama, S. Tsuruya, *Ind. Eng. Chem. Res.*, **2006**, 45, 8837-8845.

Table S3. Specific surface areas and coke contents of the pre-activated catalysts.

Catalyst	3Ag/Ti-powder	3Co ₃ O ₄ /Ti-powder	3Ag-3Co ₃ O ₄ /Ti-powder
SSA (m ² /g)	1.3	1.3	1.5
Coke content ^a (wt%)	0.3	0.2	0.6

^aCoke contents were determined by TG.

Table S4. Specific surface areas, coke contents, and particle sizes of Ag and Co-species (Co_3O_4 or CoO) of the used catalysts.

Catalyst	SSA (m^2/g)	Coke content ^c (wt%)	D_{Ag}^d (nm)	D_{Co}^e (nm)
3Ag-3 Co_3O_4 /Ti-powder ^a	1.4	0.2	36	12
3Ag-3CoO/Ti-powder ^b	1.5	0.9	38	11

^aThe fresh catalyst 3Ag-3 Co_3O_4 /Ti-powder was directly tested at 240 °C (the main phase is Ag- Co_3O_4).

^bThe fresh catalyst 3Ag-3 Co_3O_4 /Ti-powder was directly tested at 280 °C (the main phase is Ag-CoO).

^cCoke contents were determined by TG.

^dParticle size of Ag is calculated by Ag(111) peak using the Scherrer equation.

^eParticle sizes of Co_3O_4 and CoO are respectively calculated by Co_3O_4 (311) and CoO(200) peaks using the Scherrer equation.

Table S5. Specific surface areas, coke contents, and particle sizes of Co-species (Co_3O_4 or CoO) of the used catalysts.

Catalyst	SSA (m^2/g)	Coke content ^c (wt%)	D_{Co} ^d (nm)
$3\text{Co}_3\text{O}_4/\text{Ti}$ -powder ^a	1.3	0.3	7.8
$3\text{CoO}/\text{Ti}$ -powder ^b	1.4	0.4	9.5

^aThe fresh catalyst $3\text{Co}_3\text{O}_4/\text{Ti}$ -powder was directly tested at 240 °C (the main phase is Co_3O_4).

^bThe fresh catalyst $3\text{Co}_3\text{O}_4/\text{Ti}$ -powder was directly tested at 280 °C (the main phase is CoO).

^cCoke contents were determined by TG.

^dParticle sizes of Co_3O_4 and CoO are respectively calculated by $\text{Co}_3\text{O}_4(311)$ and $\text{CoO}(200)$ peaks using the Scherrer equation.

Table S6. The turnover frequencies (TOFs) of benzyl alcohol oxidation over the catalysts based on the diameter of Ag NPs^a.

Catalyst	V _{total} ^b (×10 ⁻⁴ , cm ³)	D _{Ag} ^c (nm)	V _{Ag-particle} ^d (nm ³)	Amount of Ag Particles (×10 ¹⁴)	S _{Ag-particle} ^e (nm ²)	S _{total} (cm ²)	Amount of Surface Ag Atoms ^e (×10 ¹⁸)	Conv. ^f (%)	N ^g (×10 ²²)	TOF (h ⁻¹)
3Ag-3CoO/Ti-powder ^h	8.58	40	16746	0.51	2512	1281	1.63	4	3.36	20612
3Ag-3CoO/Ti-powder ⁱ	8.58	40	16746	0.51	2512	1281	1.63	2.9	2.48	15225
3Ag/Ti-powder ^h	8.58	38	14358	0.60	2267	1360	1.73	1.1	0.91	5288
3Ag/Ti-powder ⁱ	8.58	38	14358	0.60	2267	1360	1.73	0.3	0.25	1445

^aFor each catalyst, 0.3 g was used in testing experiments; ^bThe total volume of Ag (V_{total}) is calculated as: silver mass (0.3 g × Ag-loading (wt%)) is divided by the silver density (10.49 g/cm³); ^cThe particle size is estimated from XRD patterns using Scherrer's equation; ^dThe silver particles are assumed as hemisphere, and the volume of single silver particle is $\pi D_{Ag}^3/12$, and the surface area is $\pi D_{Ag}^2/2$; ^eThe distance between the adjacent silver atoms is 0.28 nm, and one Ag atom occupies the surface area of 0.0784 (0.28 × 0.28 = 0.0784) nm²; ^fThe weight hourly space velocity (WHSV) = 500 h⁻¹, and 150 g benzyl alcohol was fed into the reactor in an hour; ^gAmount of converted benzyl alcohol (Take the converted benzyl alcohol over the catalyst 3Ag-3CoO/Ti-powder as example: the converted benzyl alcohol in one hour is 6 g (150 × 0.04 = 6 g), and the converted amount of benzyl alcohol molecule is 3.36×10^{22} (6 (g) ÷ 108 (g/mol) = 0.0556 mol; 0.0556 × 6.02 × 10²³ = 3.36×10^{22})); ^h240 °C; ⁱ220 °C.

Table S7. The turnover frequencies (TOFs) of benzyl alcohol oxidation over the catalysts based on the dispersion of Ag NPs^a.

Catalyst	D _{Ag} ^b (nm)	Dispersion ^c	Amount of Surface Ag Atoms ^d ($\times 10^{18}$)	Conv. ^e (%)	N ^f ($\times 10^{22}$)	TOF (h ⁻¹)
3Ag-3CoO/Ti-powder ^g	40	0.025	1.25	4	3.36	26880
3Ag-3CoO/Ti-powder ^h	40	0.025	1.25	2.9	2.48	19840
3Ag/Ti-powder ^g	38	0.026	1.30	1.1	0.91	7000
3Ag/Ti-powder ^h	38	0.026	1.30	0.3	0.25	1923

^aFor each catalyst, 0.3 g was used in testing experiments; ^bThe particle size is estimated from XRD patterns using Scherrer's equation; ^cThe silver dispersion is $1/D_{Ag}$; ^dAmount of Surface Ag atoms: catalyst weight \times Ag content \times dispersion $\times 6.02 \times 10^{23}$ /Molecular weight of Ag; ^eThe weight hourly space velocity (WHSV) = 500 h⁻¹, and 150 g benzyl alcohol was fed into the reactor in an hour; ^fAmount of converted benzyl alcohol (Take the converted benzyl alcohol over the catalyst 3Ag-3CoO/Ti-powder as example: the converted benzyl alcohol in one hour is 6 g ($150 \times 0.04 = 6$ g), and the converted amount of benzyl alcohol molecule is 3.36×10^{22} ($6 \text{ (g)} \div 108 \text{ (g/mol)} = 0.0556 \text{ mol}$; $0.0556 \times 6.02 \times 10^{23} = 3.36 \times 10^{22}$)); ^g240 °C; ^h220 °C.

Table S8. The turnover frequencies (TOFs) of benzyl alcohol oxidation over the catalysts based on the diameter of CoO NPs^a.

Catalyst	V_{total}^b ($\times 10^{-4}$, cm ³)	D_{CoO}^c (nm)	$V_{\text{CoO-particle}}^d$ (nm ³)	Amount of CoO Particles ($\times 10^{14}$)	$S_{\text{CoO-particle}}^e$ (nm ²)	S_{total} (cm ²)	Amount of Surface CoO Atoms ^e ($\times 10^{18}$)	Conv. ^f (%)	N^g ($\times 10^{22}$)	TOF (h ⁻¹)
3Ag-3CoO/Ti-powder ^h	13.02	13	574	22.68	265	6010	6.29	4	3.36	5341
3Ag-3CoO/Ti-powder ⁱ	13.02	13	574	22.68	265	6010	6.29	2.9	2.48	3942
3CoO/Ti-powder ^h	13.02	11	348	37.4	190	7106	7.44	0.9	0.756	1016
3CoO/Ti-powder ⁱ	13.02	11	348	37.4	190	7106	7.44	0.4	0.336	452

^aFor each catalyst, 0.3 g was used in testing experiments; ^bThe total volume of CoO (V_{total}) is calculated as: CoO mass (0.3 g \times CoO-loading (wt%)) is divided by the CoO density (6.45 g/cm³); ^cThe particle size is estimated from XRD patterns using Scherrer's equation; ^dThe CoO particles are assumed as hemisphere, and the volume of single CoO particle is $\pi D_{\text{CoO}}^3/12$, and the surface area is $\pi D_{\text{CoO}}^2/2$; ^eOne CoO occupies the surface area of 0.0955 ($0.25 \times (0.25+0.132) = 0.0955$) nm²; ^fThe weight hourly space velocity (WHSV) = 500 h⁻¹, and 150 g benzyl alcohol was fed into the reactor in an hour; ^gAmount of converted benzyl alcohol; ^h240 °C; ⁱ220 °C.

Table S9. Reaction rates of the catalysts^a.

Catalyst	Surface area (m ² /g)			T ^e (°C)	Conv. ^f (%)	N ^g (mmol)	Reaction rate (mmol/m ² h)		
	SSA ^b	S _{Ag} ^c	S _{CoO} ^d				R _{SSA} ^h	R _{Ag} ⁱ	R _{CoO} ^j
3Ag-3CoO/Ti-powder	1.5	0.42	2.00	240	4	55	122	436	91.5
3Ag-3CoO/Ti-powder	1.5	0.42	2.00	220	2.9	40	89	317	66.5
3Ag/Ti-powder	1.3	0.45	-	240	1.1	15.3	39	113	-
3Ag/Ti-powder	1.3	0.45	-	220	0.3	4.1	10.5	30.2	-
3CoO/Ti-powder	1.3	-	2.36	240	0.9	12.3	31.5	-	17.3
3CoO/Ti-powder	1.3	-	2.36	220	0.4	5.46	14	-	7.71

^aFor each catalyst, 0.3 g was used in testing experiments and WHSV is 500 h⁻¹; ^bSpecific surface area of the catalyst; ^cSurface area of Ag NPs; ^dSurface area of CoO NPs; ^eReaction temperature; ^fbenzyl alcohol conversion; ^gNumber of converted benzyl alcohol; ^hReaction rate based on the surface area of the catalyst; ⁱReaction rate based on the surface area of Ag NPs; ^jReaction rate based on the surface area of CoO NPs.

Table S10. Stability of the catalysts used in the gas phase selective oxidation of benzyl alcohol to benzaldehyde.

Catalyst	Reaction temperature (°C)	Benzyl alcohol conversion (%)	Benzaldehyde selectivity (%)	Single run life time (h)
3Ag-3Co ₃ O ₄ /Ti-powder ^a	240	90-94	97-99	150
3Ag-3Co ₃ O ₄ /Ti-powder ^b	240	92-94	97-99	300
Ag/HMS ^[1]	320	99	96	5
Ag/Ni-fiber ^[2]	300	94-97	97-98	20
AgCu/SiC-powder ^[3]	280	95-99	98-99	140

^aThe fresh catalyst 3Ag-3Co₃O₄/Ti-powder pre-activated at 380 °C.

^bThe fresh catalyst 3Ag-3Co₃O₄/Ti-powder reduced at 300 °C.

[1] J. Jia, S. Zhang, F. Gu, Y. Ping, X. Guo, Z. Zhong, F. Su, *Micropor. Mesopor. Mat.*, **2012**, 149, 158-165.

[2] M. Deng, G. Zhao, Q. Xue, L. Chen, Y. Lu, *Appl. Catal. B: Environ.*, **2010**, 99, 222-228.

[3] L. Zhao, L. Kong, C. Liu, Y. Wang, L. Dai, *Catal. Commun.*, **2017**, 98, 1-4.

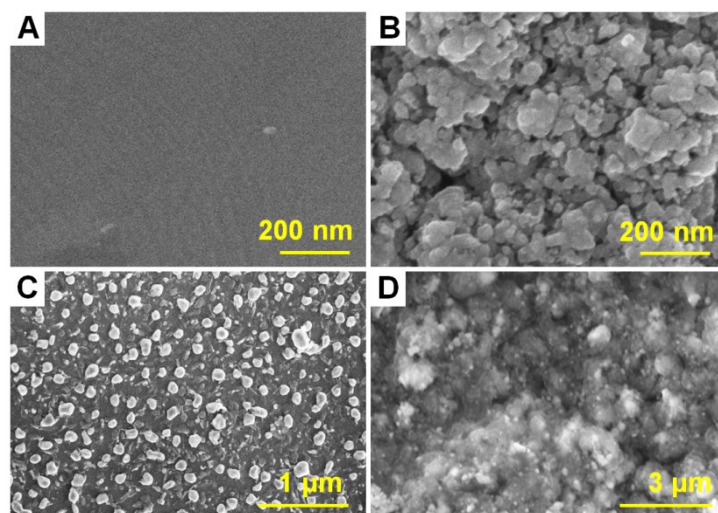


Fig. S1. SEM images of (A) pristine Ti-powder with smooth surface, (B) $3\text{Co}_3\text{O}_4/\text{Ti}$ -powder with rough surface, (C) $3\text{Ag}/\text{Ti}$ -powder with light Ag NPs on Ti-powder smooth surface, (D) $3\text{Ag}-3\text{Co}_3\text{O}_4/\text{Ti}$ -powder. Based on the SEM images in (A-C), it is clear that the amorphous substance with darker contrast level in (D) should be attributed to Co_3O_4 , and the light spots should be attributed to Ag NPs.

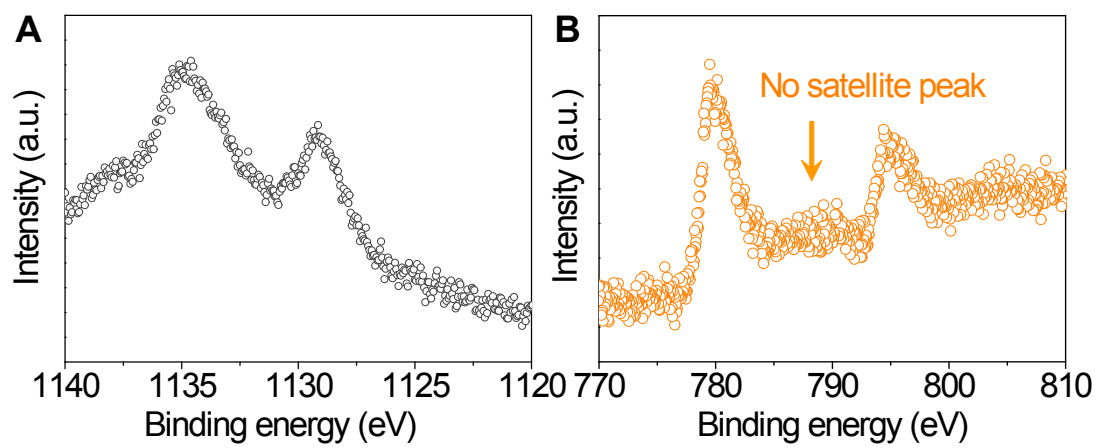


Fig. S2. (A) Ag MVV spectrum of 3Ag/Ti-powder; (B) Co 2p spectrum of 3CoO_x/Ti-powder.

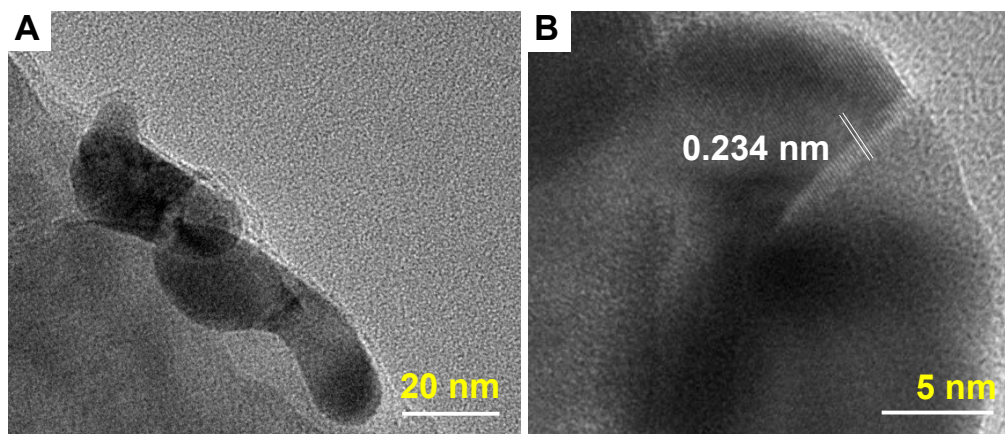


Fig. S3. (A) TEM and (B) HRTEM images of the 3Ag/Ti-powder.

Note: For the fresh 3Ag/Ti-powder and 3Ag-3CoO_x/Ti-powder catalysts, their XRD patterns show that the Ag particle sizes of these two catalysts are about 30-50 nm, but their SEM images show that the particle sizes are about 100 nm (Fig. 1A,E). From the TEM images, we could see that four or five Ag NPs gather together to form the ensembles of about 100 nm (Fig. 1H and Fig. S3A). As for the Co-species in 3Co₃O₄/Ti-powder and 3Ag-3Co₃O₄/Ti-powder (Figs. 1I,5D), the particle sizes of Co₃O₄ and CoO are not easy to be estimated due to its amorphous feature, and thus the particle sizes of Co-species are estimated by XRD to be about 10 nm.

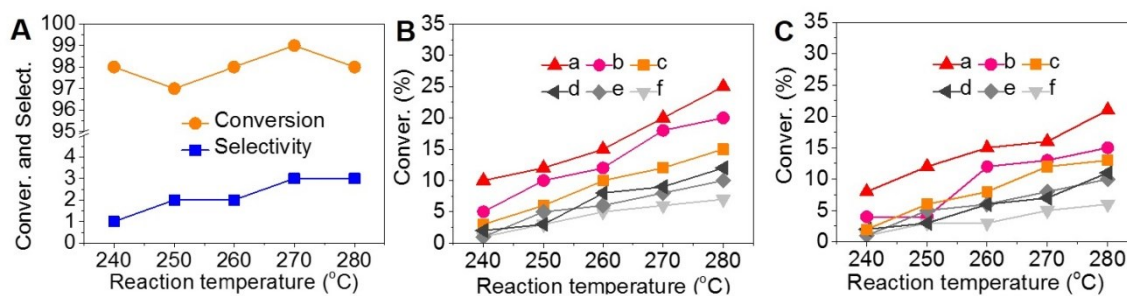


Fig. S4. (A) Benzyl alcohol conversion and benzaldehyde selectivity of the pure Ti-powder; Benzyl alcohol conversions of (B) the catalysts with pre-activation and (C) the ones without pre-activation (a, 5Ag/Ti-powder; b, 3Ag/Ti-powder; c, 1Ag/Ti-powder; d, 5Co₃O₄/Ti-powder; e, 3Co₃O₄/Ti-powder; f, 1Co₃O₄/Ti-powder).

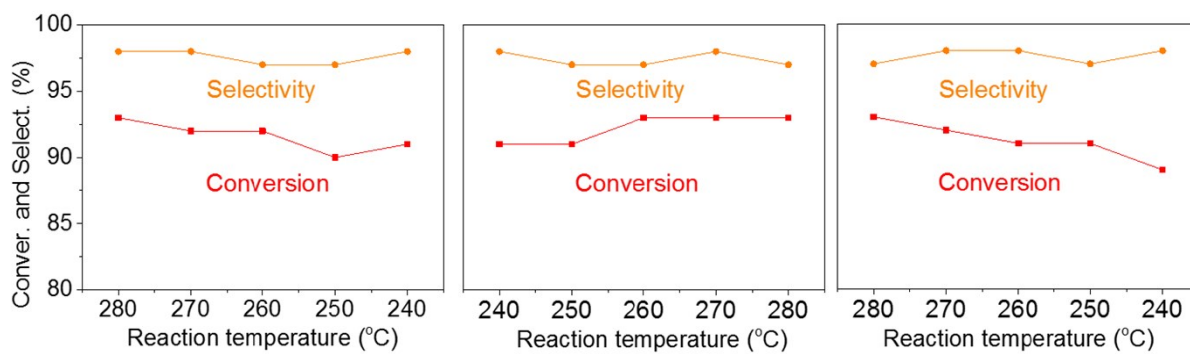


Fig. S5. Catalytic performances of the pre-activated 3Ag-3Co₃O₄/Ti-power in the cooling-heating-cooling processes.

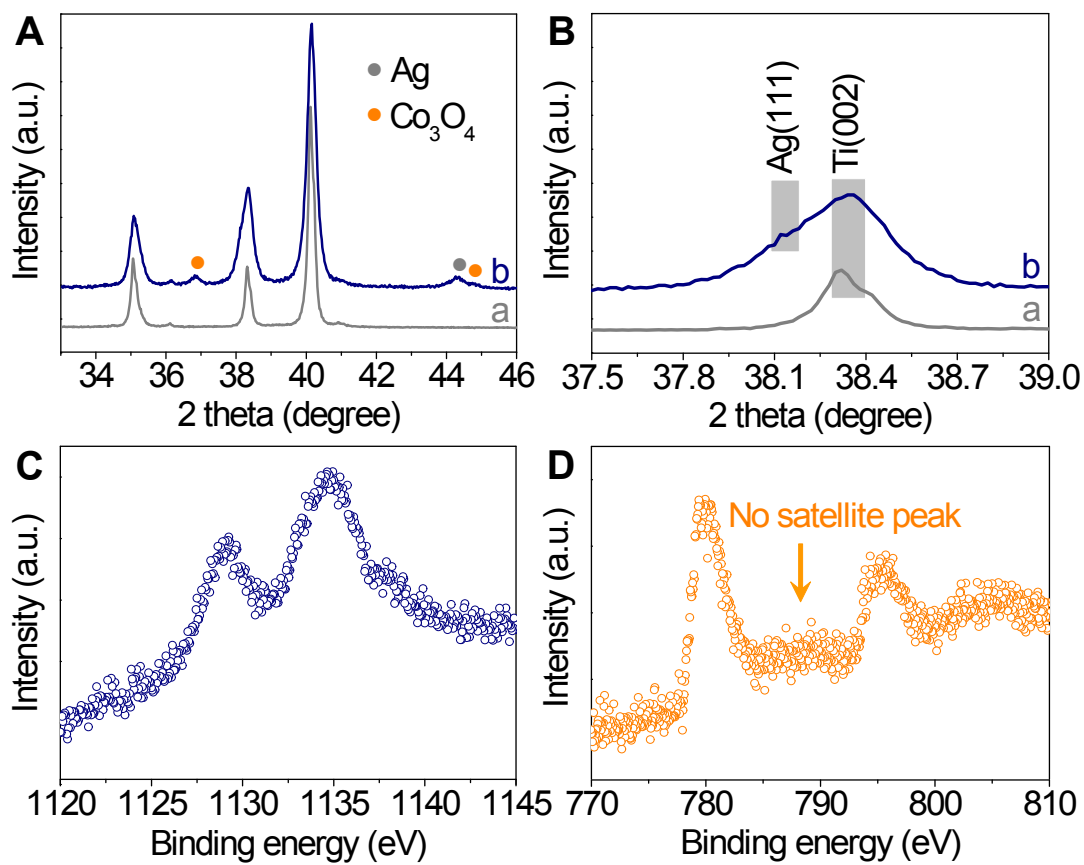


Fig. S6. (A) XRD patterns and (B) the as-amplified part of the catalysts (a, Ti-powder, b, un-activated 3Ag-3 Co_3O_4 /Ti-powder); (C) Ag MVV and (D) Co 2p spectra of the un-activated 3Ag-3 Co_3O_4 /Ti-powder.

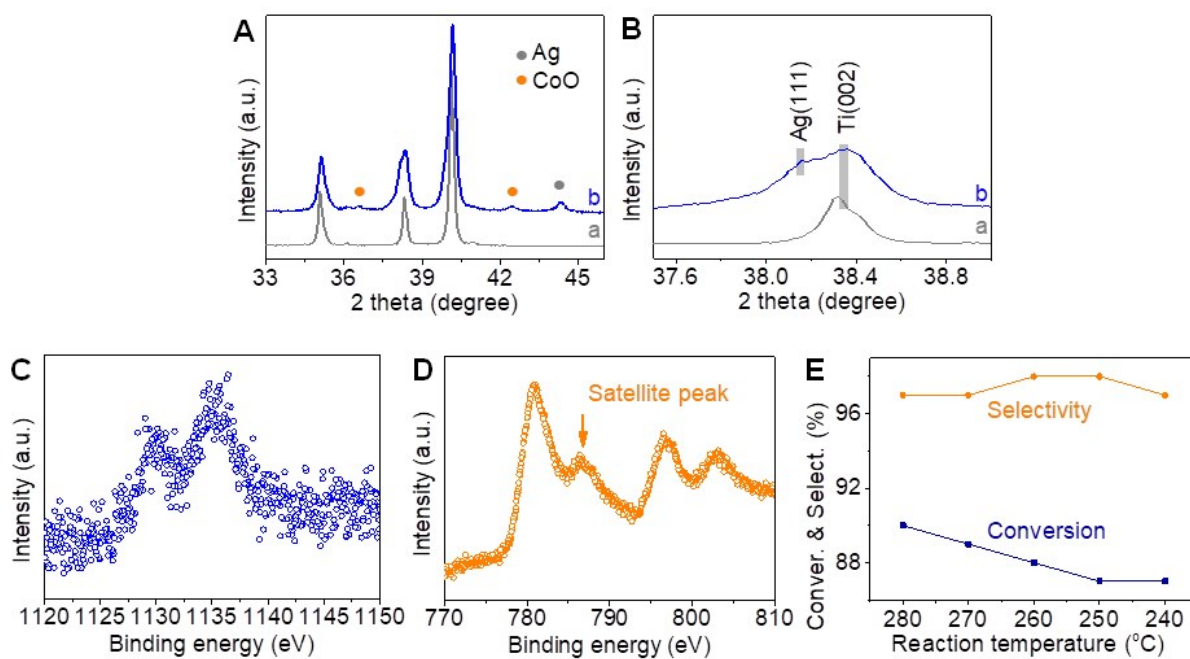


Fig. S7. (A) XRD patterns and (B) the as-amplified part of the catalysts (a: Ti-powder, b: un-activated 3Ag-3Co₃O₄/Ti-powder after 280 °C testing); (C) Ag MVV spectrum, (D) Co 2p spectrum, and (E) benzyl alcohol conversion and benzaldehyde selectivity of the un-activated 3Ag-3Co₃O₄/Ti-powder directly after 280 °C testing.

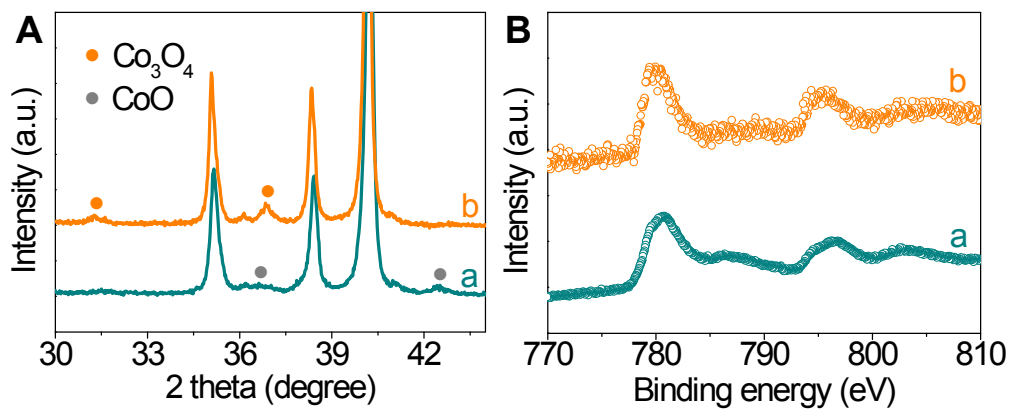


Fig. S8. (A) XRD patterns and (B) Co 2p spectra of the $3\text{Co}_3\text{O}_4/\text{Ti}$ -powder after testing at different temperatures (a, 280 °C; b, 240 °C).

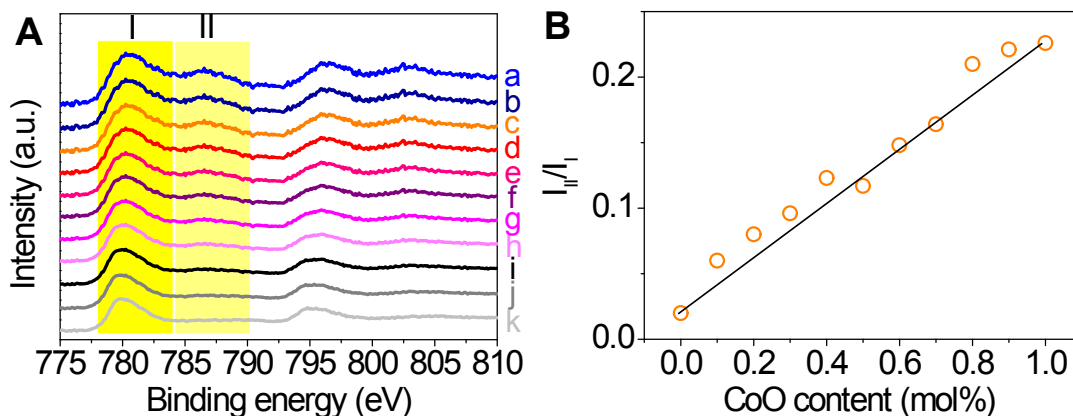


Fig. S9. (A) Co 2p spectra of the mixture of Co_3O_4 and CoO (the molar ratio of CoO/ Co_3O_4 : a, CoO; b, 9/1; c, 8/2; d, 7/3; e, 6/4; f, 5/5; g, 4/6; h, 3/7; i, 2/8; j, 1/9; k, Co_3O_4); (B) Intensity ratio of peak I to peak II (in A; denoted as $I_{\text{I}}/I_{\text{II}}$) versus CoO content (*i.e.*, $\text{CoO}/(\text{CoO} + \text{Co}_3\text{O}_4)$).

Note: In order to further estimate the CoO content in the reduced catalysts in *Section 3.3.3*, we conducted the XPS analysis for the mixture of CoO and Co_3O_4 . We could see the $I_{\text{I}}/I_{\text{II}}$ value is increased with raising the CoO content and there is a linear relationship between the $I_{\text{I}}/I_{\text{II}}$ and CoO content. So the CoO content in the catalyst reduced at 200 °C is calculated as the results mentioned above.

Part I: Quantitative analyses of O₂-TPD results

In order to determine the amount of as-desorbed O₂, the O₂ pulse experiment was conducted. One should be noted is that the chemisorption apparatus (ChemBET Pulsar TPR/TPD) records the curves of O₂-TPD based on the temperature (X axis) and the TCD signal (Y axis), while records the profile of O₂ pulse according to the time (X axis) as well as the TCD signal (Y axis). So we convert the temperature (°C, X axis) in Fig. 6 to time (s, X axis). O₂ of 0.0098 mL corresponds to the peak area of 42, and the quantitative analyses are listed as follows:

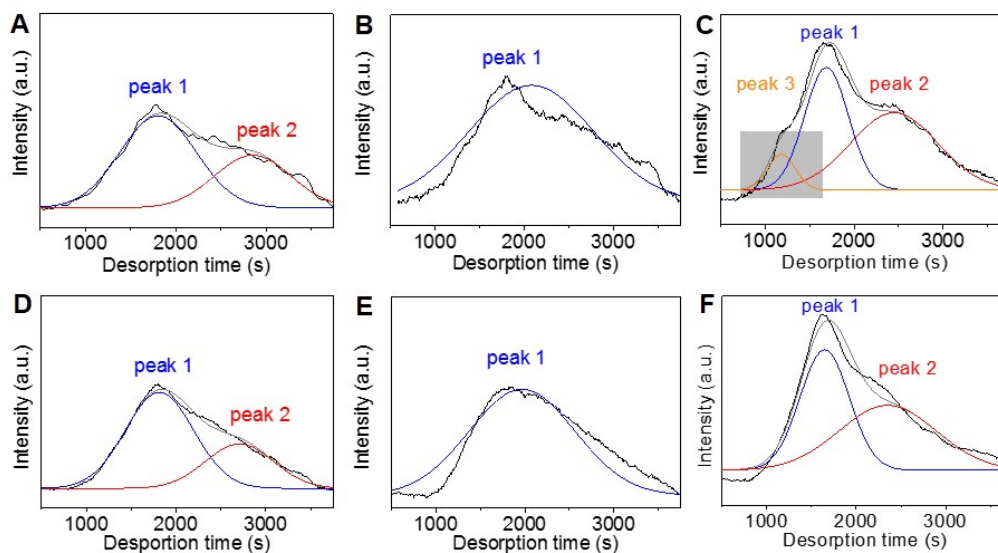


Fig. S10. The transformed O₂-TPD spectra in Fig. 6 fitted using the PEAKFIT programs for the catalysts ((A-C) used 3CoO/Ti-powder, 3Ag/Ti-powder, and 3Ag-3CoO/Ti-powder running in the presence of O₂ for 0.5 h; (D-F) the used 3CoO/Ti-powder, 3Ag/Ti-powder, and 3Ag-3CoO/Ti-powder running in the absence of O₂ for 0.5 h). Note: the desorption time from 0 to 3000 s corresponds to the temperature from 200-950 °C.

Table S11. Quantitative analyses of the oxygen species derived from O₂-TPD profiles.

Catalyst	Content of oxygen species (Temperature)		
	Peak 1	Peak 2	Peak 3
	(mmol/g) (°C)	(mmol/g) (°C)	(mmol/g) (°C)
3CoO/Ti-powder	0.1730 (630)	0.0992 (750)	-
3CoO/Ti-powder ^a	0.1645 (635)	0.0799 (750)	-
3Ag/Ti-powder	0.2532 (625)	-	-
3Ag/Ti-powder ^a	0.2204 (635)	-	-
3Ag-3CoO/Ti-powder	0.1503 (628)	0.1878 (739)	0.0272 (530)
3Ag-3CoO/Ti-powder ^a	0.1654 (625)	0.1760 (735)	-

^aThe catalysts run in the absence of O₂ for 0.5 h.

From Section 3.5.1 in the manuscript, we know that the benzyl alcohol conversions are very low for 3CoO/Ti-powder and 3Ag/Ti-powder irrespective of O₂ supplement. So the variation of the oxygen species attributed to peak 1 or 2 is not vital to the catalytic activities. However, peak 3 is absent with benzyl alcohol conversion decreasing from 92% to below 1% for 3Ag-3CoO/Ti-powder after switching-off O₂, so the active oxygen species at 530 °C plays an important role in this reaction and the amount of this active oxygen species is 0.0272 mmol/g. The similar desorption temperature of the active oxygen species is also found for our previous Au/Ni-fiber catalyst [1].

[1] G. Zhao, J. Huang, Z. Jiang, S. Zhang, L. Chen, Y. Lu, *Appl. Catal. B: Environ.*, **2013**, 140-141, 249.

Part II: Quantitative analyses of H₂-TPR results

In order to determine the amount of H₂ consumed in TPR experiments, the H₂ pulse experiment was conducted. One should be noted is that the chemisorption apparatus (ChemBET Pulsar TPR/TPD) records the curves of H₂-TPR based on the temperature (X axis) and the TCD signal (Y axis), while records the profile of H₂ pulse according to the time (X axis) as well as the TCD signal (Y axis). So we convert the temperature (°C, X axis) in Fig. 7C to time (s, X axis). H₂ of 0.0224 mL corresponds to the peak area of 250, and the quantitative analyses are listed as follows:

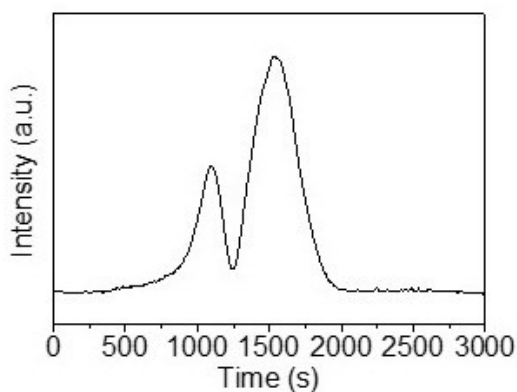


Fig. S11. The transformed H₂-TPR profile in Fig. 7C (for the fresh 3Ag-3Co₃O₄/Ti-powder, the heating rate is 10 °/min and the temperatures at 1100 and 1538 s are 250 and 340 °C, respectively).

The peak areas at 1100 s and 1538 s are 9020 and 28750 respectively, so the amount of H₂-consumption for the peak at 1100 s and the peak at 1538 s are 0.036 and 0.115 mmol. Therefore, the former peak is attributed to the reduction of Co₃O₄ to CoO, and the second one should be to the CoO reduction to metallic Co given to the fact that the theoretical H₂-consumption ratio for Co₃O₄→CoO to CoO→Co is 1/3.